A&A 473, 501–510 (2007)
DOI: 10.1051/0004-6361:20065470

Astronomy & Astrophysics

Magnetic braking in young late-type stars

The effect of polar spots

A. Aibéo[1,2], J. M. Ferreira[1,3], and J. J. G. Lima[1,4]

[1] Centro de Astrofísica, Universidade do Porto, Rua das Estrelas, 4150-762 Porto, Portugal
e-mail: aaibeo@demgi.estv.ipv.pt
[2] Escola Superior de Tecnologia de Viseu, Viseu, Portugal
[3] Universidade dos Açores, Angra do Heroísmo, Açores, Portugal
[4] Departamento de Matemática Aplicada, Faculdade de Ciências, Universidade do Porto, Portugal

Received 20 April 2006 / Accepted 26 May 2007

ABSTRACT

Context. The existence of rapidly rotating cool stars in young clusters implies a reduction of angular momentum loss rate for a certain period of the star's early life. Recently, the concentration of magnetic flux near the poles of these stars has been proposed as an alternative mechanism to dynamo saturation in order to explain the saturation of angular momentum loss.
Aims. In this work we study the effect of magnetic surface flux distribution on the coronal field topology and angular momentum loss rate. We investigate if magnetic flux concentration towards the pole is a reasonable alternative to dynamo saturation.
Methods. We construct a 1D wind model and also apply a 2-D self-similar analytical model, to evaluate how the surface field distribution affects the angular momentum loss of the rotating star.
Results. From the 1D model we find that, in a magnetically dominated low corona, the concentrated polar surface field rapidly expands to regions of low magnetic pressure resulting in a coronal field with small latitudinal variation. We also find that the angular momentum loss rate due to a uniform field or a concentrated field with equal total magnetic flux is very similar. From the 2D wind model we show that there are several relevant factors to take into account when studying the angular momentum loss from a star. In particular, we show that the inclusion of force balance across the field in a wind model is fundamental if realistic conclusions are to be drawn from the effect of non-uniform surface field distribution on magnetic braking. This model predicts that a magnetic field concentrated at high latitudes leads to larger Alfvén radii and larger braking rates than a smoother field distribution.
Conclusions. From the results obtained, we argue that the magnetic surface field distribution towards the pole does not directly limit the braking efficiency of the wind.

Key words. stars: late-type – stars: magnetic fields – stars: winds, outflows – stars: starspots

1. Introduction

Rapidly rotating cool stars have a surface magnetic flux distribution significantly different from that observed on the Sun. Doppler imaging, and more recently, Zeeman Doppler imaging, gives clear evidence for spots and significant surface magnetic flux at high latitudes (e.g. Donati et al. 1999). In many cases, a large spot, or cluster of spots, is present at the pole (Vogt & Penrod 1983; Strassmeier 2002). But clearly, spots and magnetic fields are also present at low latitudes (e.g. Barnes et al. 1998). Knowledge of the large-scale coronal magnetic topology can in principle be obtained by extrapolating magnetic fields from the boundary data (e.g. Hussain et al. 2001). However, the absence of information from a fraction of the stellar surface and the weak correlation between spots and magnetic signatures makes us look on the results of this promising technique with some caution.

The presence of spots and surface magnetic flux at high latitudes has important consequences for several phenomena occurring in the stellar corona. It can cause non-solar type phenomena like flares and X-ray emission at high latitudes (Schmitt & Favata 1999) and slingshot prominences (Collier Cameron & Robinson 1989). Here, we concentrate our attention on its implications for stellar spindown.

Wind magnetic braking is based on the principle that when gas emitted from a star is kept co-rotating with the star by magnetic torque, it transports significantly more angular momentum outwards than gas that conserves its angular momentum as it moves outwards (Schatzman 1962). In axisymmetric winds the angular momentum loss rate is equivalent to that carried by the gas kept in co-rotation with the star out to the the Alfvén surface, where the poloidal wind velocity equals the poloidal Alfvén velocity. The presence of rapidly rotating late-type stars in young clusters implies that there must be some limitation to the efficiency of magnetic braking during the pre-main sequence phase (e.g. Barnes & Sofia 1996). One possibility is that beyond some rotation rate the magnetic field strength no longer increases with increasing rotation rate, i.e., the dynamo saturates (MacGregor & Brenner 1991). But several alternatives to dynamo saturation have been suggested. These include, the increase of the closed field region with rotation rate (Mestel & Spruit 1987), and the concentration of magnetic flux near the poles of rapidly rotating stars (Solanki et al. 1997; Buzasi 1997) can lead to a saturation in the angular momentum loss rate. The effect of the closed field

region, or dead zone, on the rate of braking has been studied in some detail for both single and binary stars (e.g. Li et al. 1994).

The idea that the concentration of magnetic flux near the poles can mimic dynamo saturation is based on basic principles. The Alfvén radius is large near the poles where the field is strong, but smaller near the equator where the field is weaker. As wind braking is mainly from the contributions of low and intermediate latitudes, the overall effect is a reduction in the braking when compared with an homogeneous surface field distribution with the same total magnetic flux. In recent studies, the classical Weber & Davis (1967) wind model is explored in detail and extended to study the effect of non-uniform surface magnetic field distribution on the angular momentum loss rate (Holzwarth 2005; Holzwarth & Jardine 2005). All these models assume that the coronal radial field has a latitudinal distribution similar to the surface radial field, i.e., the force balance across the field is neglected.

In the particular case of the Sun, Ulysses observations have shown that there is no significant gradient in latitude in the radial component of the interplanetary magnetic field (Balogh et al. 1995; Smith & Balogh 1995). These observations have been explained as a result of the low plasma beta of the solar corona so that the latitudinal and longitudinal gradients in radial fields relax quickly, creating an essentially uniform field by 5–10 $R_\odot$ (Suess & Smith 1996).

In the present work we consider whether polar magnetic flux concentration towards the pole is a valid alternative to dynamo saturation as an explanation for angular momentum loss saturation. The aim of this paper is also to demonstrate that the inclusion of force balance across the field in a wind model is fundamental if realistic conclusions are to be drawn from the effect of non-uniform surface field distribution on magnetic braking. Section 2 presents a 1D Weber & Davis type wind model along a totally opened potential magnetic field resulting from a surface flux distribution concentrated towards the pole. In Sect. 3 the 2D wind model of Lima et al. (2001) is used to study the effect of the variation of surface flux with latitude on the rate of magnetic braking. The implications and limitations of the results obtained are discussed in Sect. 4 and the conclusions presented in Sect. 5.

2. Application of a 1D wind model

Present models of the inhibition of the angular momentum loss by polar concentration of the magnetic field are qualitative in nature and neglect force balance across the field (Solanki et al. 1997; Buzasi 1997; Holzwarth 2005). They are based on the assumption that the concentration of magnetic field at high latitudes generates a large Alfvén radius near the pole and a small Alfvén radius near the equator leading to a smaller effective Alfvén radius and therefore a reduced braking efficiency.

Ignoring force balance across the field and the indirect effect of the magnetic field on the wind dynamics are too severe restrictions present in these qualitative models. This makes us doubt the conclusion that field concentration at high latitudes significantly reduces the effective Alfvén radius and angular momentum loss rate. Therefore, we present a simple wind model akin to these qualitative models (Weber & Davis 1967; Sakurai 1985; Holzwarth 2005) for a surface field concentrated towards high latitudes but where force balance across field lines is partially taken into account. In modelling the solar corona and solar wind it is common to apply the potential field source surface model of the coronal magnetic field (Altschuler & Newkirk 1969; Suess & Smith 1996). In this model, the magnetic field is assumed to be potential between the surface and a spherical outer surface where the field is required to become radial. Although this model ignores volume and surface currents, it would be adequate to show that the latitudinal gradients of the radial field are smoothed out at relatively short distances from the surface (e.g. Suess et al. 1977; Riley et al. 2006). However, this model would be inadequate to determine the field configuration outside the source surface and useless if one assumes the field to be totally open. Therefore, we use a different model to determine the coronal magnetic field.

We construct a totally open magnetic field configuration by considering the magnetic field to be the dominant force in the low corona so that it is potential everywhere except at an equatorial current sheet. We then solve the wind equations along the field lines and compare our solutions with those that result from a uniform surface field.

We start by considering an axisymmetric poloidal magnetic field in an atmosphere with negligible mass and pressure. To allow for the effect of the wind without directly solving the complicated set of equations, a certain amount of magnetic flux is taken as open. We then make use of a family of analytical solutions to construct axisymmetric, partially open magnetic fields that are potential everywhere except on a force-free equatorial current sheet (Low 1986; Lepeltier & Aly 1996). The magnetic field can be expressed in spherical coordinates in terms of the stream function A:

$$\boldsymbol{B} = \frac{1}{r\sin\theta}\left(\frac{1}{r}\frac{\partial A}{\partial \theta}, -\frac{\partial A}{\partial r}, 0\right), \tag{1}$$

so that Maxwell's equation $\boldsymbol{\nabla}.\boldsymbol{B} = 0$ is satisfied. In this way, magnetic field lines are represented by contours of constant values of the stream function, A. The stream function is given by a linear combination of basic functions Z_n

$$A = \sum_n \gamma_n Z_n, \tag{2}$$

where n takes odd values, γ_n are constant coefficients and the analytical functions Z_n are developed from the oblate spheroidal harmonics and classified according to the harmonic order n. There is a free parameter, a, representing the radial distance beyond which the magnetic field is completely open. Because these functions are not orthogonal, it is complicated to determine the coefficients γ_n for a prescribed boundary condition. Nevertheless, we can combine different functions with suitable coefficients to obtain a field with the desired properties. The procedure to determine the different Z_n is described in Low (1986) where Z_1 an Z_3 are explicitly given. The functions Z_5 and Z_7 are given in Appendix A. We consider the case $A_{\rm dip} = \gamma_1^{\rm dip} Z_1$, representing a dipole-like field and $A_{\rm polar} = \gamma_1 Z_1 + \gamma_3 Z_3 + \gamma_5 Z_5 + \gamma_7 Z_7$, representing a magnetic field concentrated at the poles. The concentrated field distribution is not intended to be a realistic field distribution but merely an extreme case of field concentration towards high latitudes used for illustrative purposes.

We consider fully open fields in accordance with the picture presented in previous works (Solanki et al. 1997; Buzasi 1997; Holzwarth & Jardine 2005). Thus, we set $a = r_0$ (where r_0 represents the stellar radius) and use the values of γ_n given in Table 1, while the value of $\gamma_1^{\rm dip}$ is determined by the condition that the total magnetic flux is the same in both cases.

Figure 1 represents the radial field strength as a function of co-latitude for different radial distances from the stellar center for the two cases considered. The latitudinal profiles of the two radial fields are very different from each other near the surface

Table 1. Coefficients γ_n for a fully open magnetic field.

	Fully open
γ_1	1.0
γ_3	-3.2×10^{-2}
γ_5	1.4×10^{-3}
γ_7	1.0×10^{-4}

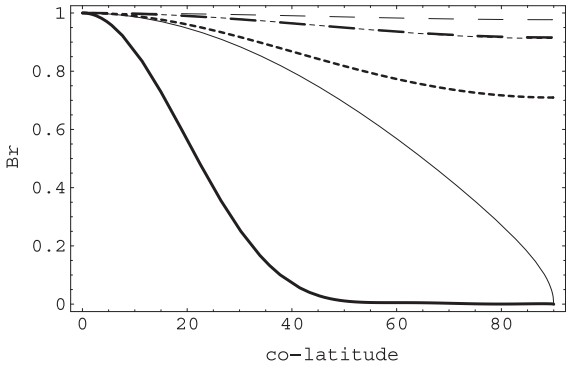

Fig. 1. Fully open fields. The radial field latitudinal distribution: at the surface (full line), at $r = 4r_0$ (short dashed) and at $r = 8r_0$ (long dashed). The thick lines represent the poleward concentrated field and the thin lines the dipole-like field. For a clearer representation all the radial fields are set to unity at the pole.

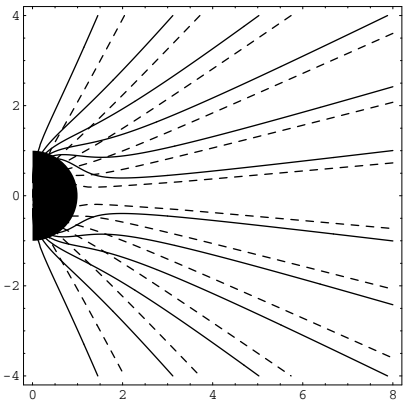

Fig. 2. Fully open fields. The lines of force of the dipole-like surface flux distribution (dashed line) and the flux distribution concentrated towards the pole (full line). For the later case notice the field lines bending towards the equator.

of the star. However, at intermediate ($r = 4r_0$) and at large distances from the surface ($r = 8r_0$) they are similar to each other and to the split monopolar field. In Fig. 2 the coronal field topology for both cases is represented. This figure clearly shows that for surface fields concentrated near the poles, the field lines that emerge at high latitudes are pushed towards low latitudes in the low corona, resulting in a field almost independent of latitude further out in the corona. It is straightforward to show, using the same model for $a > r_0$, that the same happens for partially open fields.

These results demonstrate that very different surface flux distributions give rise to similar coronal fields. Physically, this is simply a consequence of the very large magnetic pressure difference between high and low latitudes (this is clearly illustrated in Parker's monograph, Parker 1979). Therefore, a strong field near the pole and a weak field near the equator at the stellar surface do not imply that the same is true in the corona. We note that, in essence, this argument is identical to the one used to explain Ulysses observations concerning the lack of latitudinal gradients in the radial component of the solar wind magnetic field (Suess & Smith 1996). Having obtained the poloidal field configuration, we now determine the polytropic wind solution along the field. We consider a star of one solar mass and radius, rotating rigidly and characterized by a corona with uniform base temperature, $T = 2.1 \times 10^6$ K, and uniform base density, $\rho = 10^{-13}$ kg/m^3. We also assume a mean atomic weight of $\tilde{\mu} = 0.6$ and a polytropic index of $\gamma = 1.15$. Here we follow closely the approach described in Sakurai (1985). In brief, we solve the Bernoulli equation presented in the Appendix B for different stellar rotation periods, ranging from 1 to 30 days, and for different total surface magnetic fluxes, corresponding to uniform fields ranging from 1 to 100 G. However, we do not assume the area of each flux tube to increase as r^2, but we impose the area variation to be that of the solution of the field. In particular, we consider two flux tubes with contrasting properties. One has its roots near the pole at latitude 89° where the field near the surface expands very rapidly, and the other has its roots close to the equator at latitude 1° where the field near the surface first contracts and then expands very slowly. Both flux tubes expand $\propto r^2$ far from the surface. The latitude of the flux tube is assumed the same and constant for all the flux tubes. We then compare the solutions obtained with those along a flux tube with an area variation $\propto r^2$. The solutions are compared imposing equal flux tube area at the Alfvén radius as the angular momentum loss rate is determined from the Alfvén radius, velocity and density (Eq. (16)). Density, velocity and radius at the Alfvénic point are denoted by ρ_*, v_* and R_*, respectively. We find that: i) the Alfvén radius changes very little ($\leq$2%), being larger for rapidly expanding loops; ii) the base velocity increases considerably as one goes from slowly expanding to rapidly expanding flux tubes (over two order of magnitude); iii) the mass loss rate at the Alfén radius changes little from flux tube to flux tube; iv) the slow magnetosonic point decreases significantly from slowly expanding to rapidly expanding loops (up to 25%); v) the differences in angular momentum carried by the wind and magnetic torques ($\propto \rho_* V_* R_*^4$) by the different flux tubes of equal area at R_* are negligible ($\leq$2%). These results determine that, in disagreement with previous results, there is no significant difference in the angular momentum loss when the surface field changes from being uniform to being concentrated towards the poles. We note that centrifugal acceleration on rapidly rotating stars is inefficient at high latitudes and generates a non-spherical Alfvén surface, but clearly, this is independent of the surface field distribution.

In the simple model presented here we observe the expansion of the polar field to low latitudes. However, this expansion can be limited by a high equatorial gas pressure and the Lorentz force due to the azimuthal magnetic field. Therefore, these particular results are only valid provided the corona near the stellar surface is a low beta plasma and the effect of the azimuthal magnetic field can be neglected, which is likely to be the case in magnetized rapidly-rotating stars. The parameters considered range from those characteristic of stars termed as slow magnetic rotators (SMR) to those characteristic of fast magnetic rotators (FMR), as classified by Belcher & MacGregor (1976). The more rapidly rotating and magnetic stars considered in the present analysis are FMR, for which there is a poleward collimation of the field lines (Heyvaerts & Norman 1989) that is neglected in these simple models. But, as will be argued in detail in Sect. 4,

this is largely independent of what is under scrutiny here – the effect of the surface magnetic flux distribution.

To complete the model just presented, two different and complementary approaches could be pursued. In one approach, numerical simulations are employed (e.g. Sakurai 1985; Keppens & Goedbloed 1999) while in the other, analytical or semi-analytical solutions of the equations are obtained under some simplifying assumptions. Several self similar non-polytropic models have been developed based on the assumption of a non-linear separation of variables (e.g. Tsinganos & Trussoni 1991; Sauty & Tsinganos 1994). Here, we adopt the analytical 2-D model of Lima et al. (2001) as it is the only available analytical model that allows us to vary the magnetic surface flux distribution and determine how it affects the wind dynamics and the angular momentum loss rate. As in the 1-D model of Holzwarth (2005), the poloidal field and velocity are purely radial, but, in this case, force balance across the field is obeyed in a self-consistent way. Although these analytical models are more rigorous than the qualitative model just presented, they require several simplifying assumptions that may be physically unrealistic or undesirable. Therefore, it seems necessary to study how such analytical models compare with qualitative models which are more commonly applied to address the problem of magnetic braking.

3. Application of a 2D wind model

3.1. A self-similar MHD wind model

In order to construct a model for an axisymmetric wind emanating from a central rotating star, Lima et al. (2001) have assumed θ-self similarity and deduced a solution of the system of ideal MHD equations. The solution is found by a non-linear separation of variables, keeping the treatment as general as possible (e.g. not assuming, a priori, any prescribed variation with latitude of the velocity, density or magnetic field).

The model uses spherical coordinates $[r, \theta, \phi]$ and assumes a simple geometry with zero meridional components of the velocity and magnetic fields in order to find a treatable form for the fundamental solutions an therefore calculate a solution. The outflow dynamics are described by the following set of equations of distance and co-latitude for the radial velocity, azimuthal velocity, radial magnetic field, azimuthal magnetic field, density, pressure and stellar angular velocity:

$$V_r(R,\theta) = V_0 Y \sqrt{\frac{1+\mu\sin^{2\epsilon}\theta}{1+\delta\sin^{2\epsilon}\theta}} \quad (3)$$

$$V_\phi(R,\theta) = \lambda V_0 \left(\frac{Y_* - Y^2}{1-M_{\rm A}^2}\right) \frac{R\sin^{\epsilon}\theta}{\sqrt{1+\delta\sin^{2\epsilon}\theta}} \quad (4)$$

$$B_r(R,\theta) = \frac{B_0}{R^2}\sqrt{1+\mu\sin^{2\epsilon}\theta} \quad (5)$$

$$B_\phi(R,\theta) = \lambda B_0 \left(\frac{R_*^2/R^2 - 1}{1-M_{\rm A}^2}\right) R\sin^{\epsilon}\theta \quad (6)$$

$$\rho(R,\theta) = \frac{\rho_0}{YR^2}\left(1+\delta\sin^{2\epsilon}\theta\right) \quad (7)$$

$$P(R,\theta) = \frac{1}{2}\rho_0 V_0^2 \left(Q_0 + Q_1\sin^{2\epsilon}\theta\right) \quad (8)$$

$$\Omega(\theta) = \frac{\lambda V_0 Y_*}{R_0}\frac{\sin^{\epsilon-1}\theta}{\sqrt{1+\delta\sin^{2\epsilon}\theta}} \quad (9)$$

where ρ_0, B_0, V_0 represent the density, radial magnetic field and radial velocity at the polar base of the wind, respectively, and $M_{\rm A}$, Q_0 and Q_1 are functions of R and Y, itself a function of R. The function $M_{\rm A}$ is the Alfvén number defined by the ratio of the poloidal velocity to the Alfvén velocity ($M_{\rm A}^2 = 4\pi\rho V_r^2/B_r^2$). From this definition and from Eqs. (3) and (5) it results that the Alfvén iso-surfaces are spherical. The calculation of the function expressing the radial dependence of the radial velocity, $Y(R)$, is made from the combination of the radial and latitudinal components of the momentum equation, which results in one first order non-linear differential equation. Such an equation, which combines force balance along and across the fieldlines, shows two points where both the numerator and denominator vanish simultaneously. These singular points are related to the non-linearity of the steady-state system of equations. The Alfvén point, where $M_{\rm A} = 1$, is a star-type singular point and it is indicated by (R_*, Y_*). All solutions can pass through it. The second singular point is the fast magnetosonic point and it is an X-type point allowing only two solutions to cross it. Due to the self-similar nature of this model, in which force balance is solved simultaneously along and across the fieldlines, the results show that there are only the above two critical points. Other self-similar wind models show the same number of critical points (e.g. Sauty & Tsinganos 1994). A detailed discussion of the nature of these critical points can be found in Tsinganos et al. (1996). The functions Q_0 and Q_1 represent, respectively, the isotropic and latitudinal dependent normalized components of the pressure (for further details on their calculation see Lima et al. 2001). The temperature is calculated a posteriori using the classical ideal gas law.

The solutions of this model are defined by six dimensionless parameters: λ, ν, $M_{\rm A}^0$, μ, δ, ϵ. The parameter λ represents the ratio between two velocities: the equatorial stellar rotation velocity and the polar radial velocity at the Alfvén point: $\lambda = r_0\Omega(R_0, \pi/2)/V_r(R_*, 0)$ (for $\delta = 0$). As a consequence of the angular momentum conservation and induction equation, this parameter can analogously be defined using the two components of the magnetic field. The parameter ν is the ratio of the stellar escape velocity and V_0. Thus, for a given value of ν, the parameter λ and Y_* define how fast or slow rotator the star is. The parameter $M_{\rm A}^0$ defines the Alfvén number at the wind base, i.e., it defines how magnetized the star is. The remaining three parameters are related to the latitudinal distribution of the different physical quantities.

The parameter δ evaluates the density anisotropy between the equator and the pole (cf. Eq. (8)). In a similar way, the parameter μ determines the radial magnetic field anisotropy between the equator and the pole (cf. Eq. (5)). Finally, ϵ controls the shape of the latitudinal distribution of the magnetic field, density, and velocity where high values lead to steep variations and low values lead to smoother variations. These three anisotropy parameters yield the flexibility of generating solutions corresponding to different latitudinal dependences and enable us to model stellar outflows showing distinct latitudinal distributions of magnetic flux.

3.2. Analysis of a typical wind solution

From a purely theoretical point of view, if the concentration of open magnetic flux reduces the efficiency of magnetic braking, then it will do so for both fast and slow rotators. Both observations and theoretical modelling indicate that a substantial amount of magnetic flux concentrates at high latitudes for solar type-stars of periods below a few days (~5 day; Strassmeier 2005; Schuessler & Solanki 1992; Schrijver & Title 2001). We then consider a young, moderately rapidly-rotating solar type

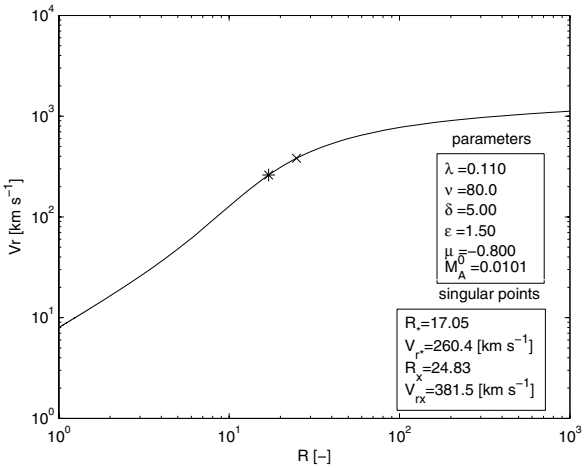

Fig. 3. A typical wind solution for a highly magnetized object in the Lima et al. (2001) model, featuring two distinct singular points: the Alfvén point and a fast magnetosonic point.

star with $r_0 = 1\,R_\odot$, $M = 1\,M_\odot$, with a 4 day period and with a coronal density $\rho_0 = 10\rho_\odot = 1.6 \times 10^{-12}$ kg/m^{-3}. The parameters adopted are: ${M_{\rm A}}^0 = 0.01$, $\nu = 80$, $\lambda = 0.11$, yielding $V_0 = 7.72\,\mathrm{km\,s^{-1}}$, $V_1 = 0.85\,\mathrm{km\,s^{-1}}$, and $B_0 = 11$ G. The parameters describing the latitudinal profiles are $\delta = 5$, $\mu = -0.8$ and $\epsilon = 1.0$ that are representative of a star with more magnetic flux at high latitudes than at low latitudes.

The wind solution obtained is presented in Fig. 3 and in order to understand what forces are relevant in accelerating the wind and in maintaining the equilibrium in the latitudinal direction, we present a detailed study of this solution.

The three components of the equation of motion, under the assumptions of axisymmetry and zero theta component's are explicitly written in Eqs. (10) to (12) where we have labelled the different terms with roman numerals for easier identification.

$$\underset{\mathrm{I}}{\rho V_r \frac{\partial V_r}{\partial r}} \underset{\mathrm{II}}{- \rho \frac{V_\phi^2}{r}} \underset{\mathrm{III}}{+ \frac{\partial p}{\partial r}} \underset{\mathrm{IV}}{+ \frac{B_\phi^2}{4\pi r}} \underset{\mathrm{V}}{+ \frac{B_\phi}{4\pi}\frac{\partial B_\phi}{\partial r}} \underset{\mathrm{VI}}{+ \frac{\rho G M}{r^2}} = 0 \qquad (10)$$

$$\underset{\mathrm{VII}}{\rho V_\phi^2 \frac{\cos\theta}{\sin\theta}} \underset{\mathrm{VIII}}{- \frac{\partial p}{\partial \theta}} \underset{\mathrm{IX}}{- \frac{B_r}{4\pi}\frac{\partial B_r}{\partial \theta}} \underset{\mathrm{X}}{- \frac{B_\phi^2}{4\pi}\frac{\cos\theta}{\sin\theta}} \underset{\mathrm{XI}}{- \frac{B_\phi}{4\pi}\frac{\partial B_\phi}{\partial \theta}} = 0 \qquad (11)$$

$$\frac{\rho V_r}{r}\frac{\partial (r V_\phi)}{\partial r} - \frac{B_r}{4\pi r}\frac{\partial (r B_\phi)}{\partial r} = 0. \qquad (12)$$

In Fig. 4 we can observe that close to the surface the dominant forces in the radial direction are the gas pressure gradient (III) and gravity (VI), which balance each other in almost hydrostatic equilibrium. Further out, at high and intermediate latitudes (panel a) of Fig. 4), it is the pressure gradient that accelerates the wind with a small contribution from the other forces. However, near the equator both the centrifugal force (II) and the Lorentz force (IV+V) due to the ϕ-component of the field are important in accelerating the wind near and beyond the singular points. This is in accordance with what one would expect for a star with the properties considered here.

It is also instructive to analyze the force balance in the θ-direction. Figure 5 shows that below the critical points the magnetic pressure gradient due to the radial magnetic field (IX) is balanced by the gas pressure gradient (VIII) and, to a lesser extent, by the Lorentz force due to the ϕ-component of the field (X+XI). The gas pressure gradient decreases and changes sign close to the Alfvén point, as indicated by the crosses on the dotted curve. In this region the force opposing the radial magnetic field pressure gradient is the Lorentz force resulting from the ϕ-component of the magnetic field (X + XI). Therefore, the expansion of the poloidal field from the high latitudes towards the low altitudes is prevented by both the gas pressure gradient and the toroidal component of the magnetic field. This is possible because the plasma β ($\beta = p/(B^2/8\pi)$) at the surface is relatively high, varying from 0.16 at the pole to 4.7 at the equator. Otherwise, in a low β corona, the field lines would bend towards regions of lower magnetic pressure so that different magnetic surface distributions would generate similar coronal topologies, as discussed in Sect. 2. Beyond the critical points, the Lorentz force that tends to collimate the field lines towards the poles (IX) is balanced by the gas pressure gradient (VII), so that the field lines remain radial in the poloidal plane. For a significantly more magnetic and more rapidly rotating star than the one considered here, there is no force capable of balancing the Lorentz force and the model cannot generate physically acceptable solutions. In other words, the assumptions of no meridional components of magnetic field and velocity and of a full open magnetic field is incompatible with a magnetically dominated low corona.

The ϕ-component of the equation of motion expresses that the change of angular momentum of the wind is equal to the magnetic torque. As a consequence, the azimuthal velocity is close to co-rotation near the surface due to the strong magnetic torque, while far from the surface this torque becomes less effective and the conservation of angular momentum implies that the azimuthal velocity must decrease proportionally to $1/R$, as is illustrated in Fig. 6.

Figure 7 represents the gas pressure and temperature at two different latitudes as a function of radial distance. The pressure close to the surface increases towards the equator but has the opposite behaviour further out, i.e., as pointed out earlier, the gas pressure gradient changes sign close to the Alfvén point. In this model, the coronal temperature increases towards the pole as a consequence of the latitudinal behaviour of the gas pressure and density. Having in mind that the temperature is not imposed but obtained a posteriori from the perfect gas law, its values of $T \approx 10^6$–10^7 K are in relatively good agreement with what we would expect for an active solar-type star. It is usually assumed in numerical models of solar and stellar winds that the corona is isothermal, or, more generally, it follows a polytropic law. In our approach it is not possible to impose this behaviour and it is also not desirable, as stellar coronae are not well described by such simple laws. Additionally, it is not expected that coronal regions of large and small magnetic field concentration have the same temperature. Instead, the temperature profile allows us to deduce, from a consistent solution of the energy equation, the regions where energy is deposited or removed

$$\sigma = V_r \frac{\partial}{\partial R}\left(\frac{P}{(\Gamma - 1)\rho}\right) + P V_r \frac{\partial}{\partial R}\left(\frac{1}{\rho}\right) \qquad (13)$$

where Γ is the ratio of specific heats and σ represents the net effect of all sources and sinks of energy per unit of mass. In the particular case of the solution presented here, the temperature varies with latitude and with radius. From Figs. 7 and 8 we can infer that the temperature and heating rate are higher at high latitudes than at low latitudes and that there must be a heating mechanism that deposits energy at large radii, beyond the sub-Alfvénic region. Although this model has no specific heating mechanism included, we note that Alfvén waves dissipation

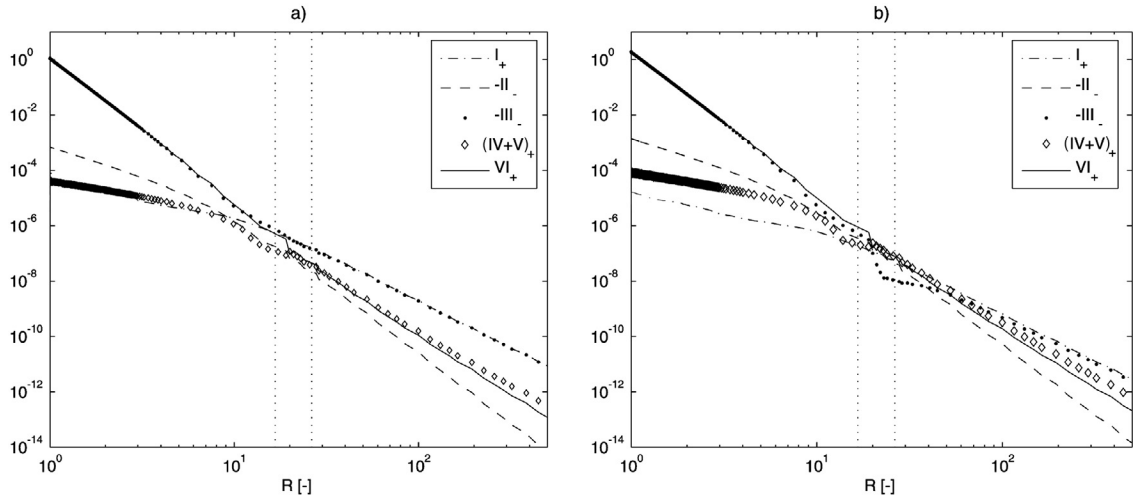

Fig. 4. Absolute values of the different terms of the radial component of the force balance equation as a function of radial distance. Positive terms are labelled by (+) and negative terms by (–). In panel **a)** at 45° of latitude. In panel **b)** at the equator.

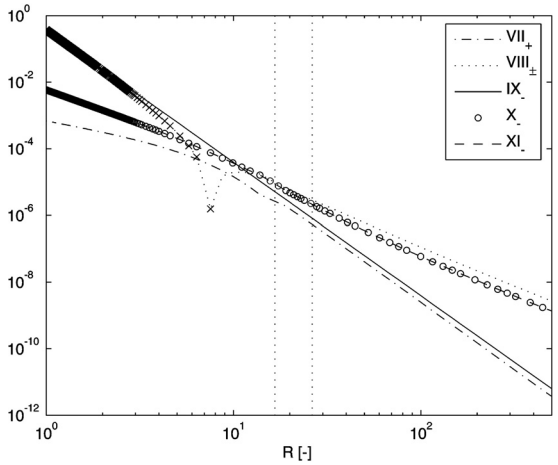

Fig. 5. Absolute values of the different terms of the θ-component of the force balance equation as a function of radial distance at the pole. Positive terms are labeled by (+), negative terms are labeled by (–) and terms that change sign by (±) together with a cross along the part where they are negative.

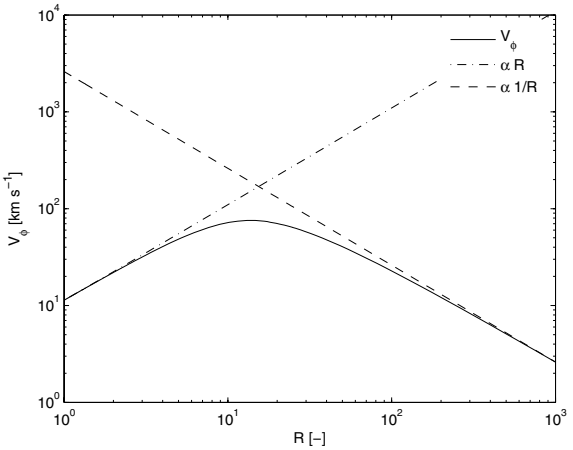

Fig. 6. Azimuthal velocity at the equator as a function of radial distance. Also represented are the profiles corresponding to co-rotation (dot-dashed line) and angular momentum conservation (dashed line)

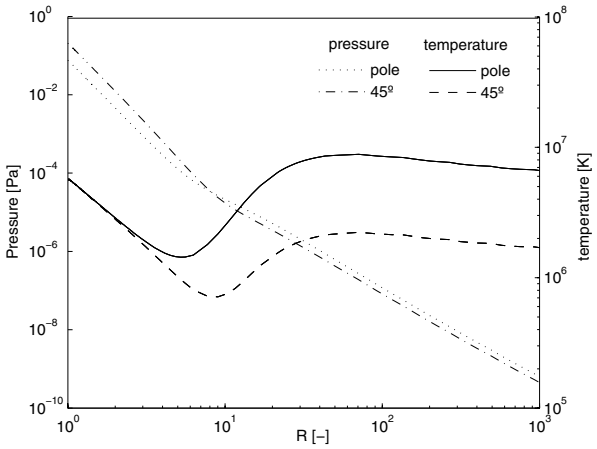

Fig. 7. Radial profiles of pressure and temperature at 45° of latitude and pole.

is a viable mechanism for energy deposition far from the surface, generating temperature profiles somewhat resembling the ones presented here (Cranmer 2005).

The exploration of the parameter space reveals some important results concerning the overall behaviour of these wind solutions. In general, an arbitrary choice of parameters of the model will not generate wind solutions. In particular for the anisotropy parameters, μ and δ have a crucial influence in the properties of the solutions. On one hand, accelerating wind solutions require the density to be higher at the equator than the pole, i.e., positive values of δ. On the other hand, there are meaningful solutions only for $\mu < 0$. If μ takes positive values, the critical solution shows a different fast magnetosonic critical point – a spiral type point, preventing any possibility of building wind-type solutions. This is shown in Fig. 9 where a comparison between a typical wind solution for a negative value of μ and a terminated solution for a positive value of μ is presented.

The effect of the different parameters on the wind solution can only be understood by taking into account force balance along the lines (radial and azimuthal components of the momentum equation, Eqs. (10) and (12)) but also from the equilibrium across the lines (θ-component of the momentum equation,

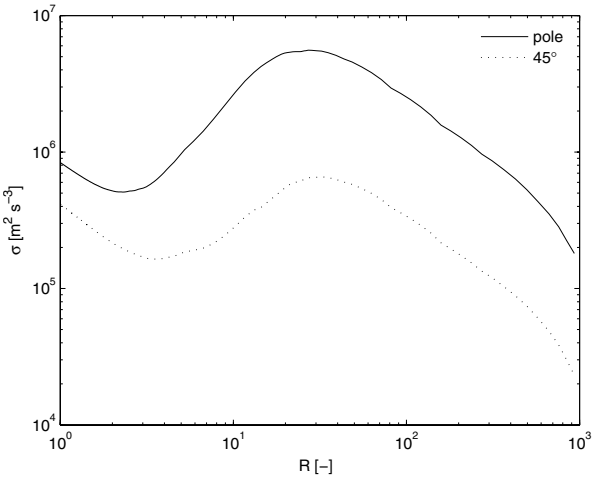

Fig. 8. Radial profile of the heating rate per unit of mass at 45° of latitude and pole.

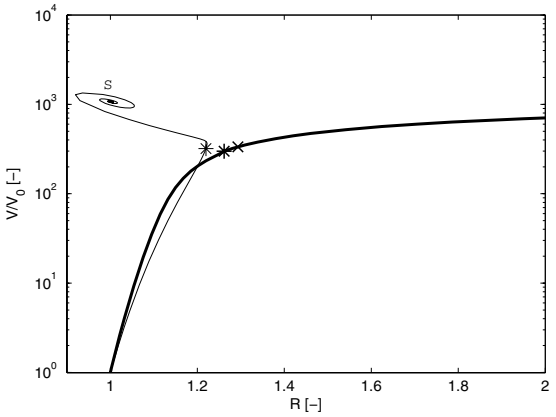

Fig. 9. Comparison between solutions for positive and negative values of the parameter μ. The solid bold line represents the solution typical topology for wind type critical solutions ($\mu = -0.05$). The narrow solid line represents the topology for solutions with positive values of μ (= 0.005), which are not wind solutions. The * markers stand for star-type points (the Alfvén points), the **x** marker represents the *x*-type point and the **s** marker points out the spiral-type critical point.

Eq. (11)). As an example, if we change the parameters in order to describe an even more magnetic and more rapidly-rotating star, we would not be able to obtain a solution. Physically, this results from lack of force balance across the field. The low gas pressure can neither balance the tendency of field lines to bend towards low latitudes at small distances from the surface, nor the tendency of field lines to collimate at large distances as required by the assumptions of the model.

A complete study of the behaviour of the wind solution with the variation of the parameters is extremely complex because the influence each parameter has on the critical solution is often dependent on the values taken by the other parameters. This particular study is beyond the scope of the present work.

3.3. Variation of angular momentum loss with the distribution of the surface field

In order to compare the angular momentum loss rate for different distributions of the magnetic field at the surface of the star, we must prescribe a fixed value of total magnetic flux, F_0. Therefore, the surface magnetic field strength at the pole must be defined accordingly:

$$B_0 = \frac{F_0}{4\pi r_0^2 \int_0^{\pi/2} \sin\theta \sqrt{1+\mu\sin^{2\epsilon}\theta}\,\mathrm{d}\theta}. \tag{14}$$

The mass loss rate per unit solid angle at co-latitude θ is

$$-\dot{m}(\theta) = \rho V_r r^2 = \rho_0 V_0 r_0^2 \sqrt{(1+\mu\sin^{2\epsilon}\theta)(1+\delta\sin^{2\epsilon}\theta)}. \tag{15}$$

The total angular momentum loss rate is equivalent to that carried by the gas kept in co-rotation with the star out to the Alfvén surface, which can be expressed as

$$-\dot{J}(\theta) = 4\pi \int_0^{\pi/2} \Omega(\theta)\rho_* V_* R_*^4 \sin^3\theta\,\mathrm{d}\theta. \tag{16}$$

Or equivalently, in terms of the model parameters (Lima et al. 2001) as

$$-\dot{J}(\theta) = \lambda r_0^3 B_0^2 \int_0^{\pi/2} \sin^{\epsilon+2}\theta \sqrt{1+\mu\sin^{2\epsilon}\theta}\,\mathrm{d}\theta. \tag{17}$$

In this model, ρ, V_r and Ω are functions of δ and yield an angular momentum loss rate that is not directly dependent on this anisotropy parameter. By changing the anisotropy parameters μ and ϵ the Alfvén radius and Alfvén velocity change.

In order to evaluate the polar concentration of a given magnetic field surface distribution, we first compare the magnetic flux at low co-latitudes (from 30° towards 0°) with the overall total flux. Thus,

$$\omega = \frac{\int_0^{\pi/6} \sqrt{1+\mu\sin^{2\epsilon}\theta}\,\mathrm{d}\theta}{\int_0^{\pi/2} \sqrt{1+\mu\sin^{2\epsilon}\theta}\,\mathrm{d}\theta}. \tag{18}$$

Then, we define the parameter τ that evaluates the magnetic field concentration towards high latitudes by comparing it with a uniform magnetic field distribution (the split-monopole case with ϵ =1 and $\mu = 0$)

$$\tau = \frac{\omega}{\omega_{\mathrm{monopole}}} = 3\frac{\int_0^{\pi/6} \sqrt{1+\mu\sin^{2\epsilon}\theta}\,\mathrm{d}\theta}{\int_0^{\pi/2} \sqrt{1+\mu\sin^{2\epsilon}\theta}\,\mathrm{d}\theta}. \tag{19}$$

If $\tau > 1$ the field is concentrated towards the pole while if $\tau < 1$ the field is concentrated towards the equator.

As a result of the way the model is constructed, a change in the parameters μ or ϵ will change the total amount of magnetic flux, the location of the Alfvén radius and also the rotation period of the star (see Eqs. (14) and (9)). Therefore, an iterative procedure on the parameters λ and M_A is performed so that the different solutions under comparison have the same total amount of magnetic flux and rotation period within an error of 5%.

By evaluating the angular momentum loss rate for different wind solutions attained for several sets of μ and ϵ, we are able to obtain a relation between the magnetic polar field concentration and the total angular momentum loss. This is shown in Fig. 10, where solid lines represent how $-\dot{J}$ varies with τ due to the variation of μ, with constant ϵ. Physically, this corresponds to determining how the variation of the magnetic field distribution with a fixed rotation profile affects the angular momentum loss rate. Also represented by dashed lines is the case of how $-\dot{J}$ varies with τ due to the variation of ϵ, with constant μ. In

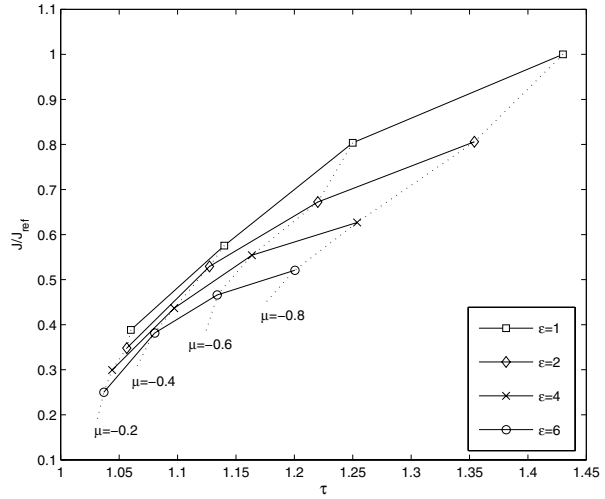

Fig. 10. Total angular momentum loss variation as a function of polar field concentration, for different sets of μ (dashed lines) and ϵ (solid lines).

this case, both the magnetic field and rotation latitudinal profiles vary. All solutions considered here are lied as SMR, revealing that centrifugal forces are not predominant for the wind acceleration mechanisms. The dynamics of the wind is, as previously shown, independent of the forces generated by the rotation of the central body. This is true even for the particular case where the period is of 4 days since other contributions, such as the pressure gradient, are more important.

Our purpose is to study young and rapidly rotating stars, therefore we must consider small values of ϵ and small values of δ, as this kind of object shows near rigid body surface rotation with a slightly faster equator (e.g. Collier Cameron & Donati 2002). Also, it is only adequate to compare stars with different surface magnetic field distribution but with the same surface rotation latitudinal profile. Thus, we restrict the physical application of this model to the cases of constant ϵ and variable μ. If we analyze the solid lines in Fig. 10, we see that the total angular momentum loss is an increasing function of τ. Therefore, the higher the magnetic field polar concentration, the more efficient magnetic braking is. Referring to Eq. (16), and noticing that, by continuity, $\rho_* V_* R_*^4 = \rho_0 V_0 R_0^2 R_*^2$, changes in total angular momentum loss must arise from changes in the mass loss rate or changes in the Alfvén radius. But as the mass loss rate decreases with increasing τ and $|\mu|$ (cf. Eq. (15)), we can conclude that the increase in total angular momentum loss is due to an increase in the Alfvén radius that more than compensates the decrease in mass loss.

As $|\mu|$ increases, B_0 increases and $M_{\rm A}^0$ decreases, i.e., at the pole the star becomes more magnetic as the field concentrates there. As $V_* R_*^2 \propto (M_{\rm A}^0)^{-2}$ we see that either the Alfvén velocity, or the Alfvén radius or both must increase. From the different solutions present in Fig. 10 as well as an analysis of the differential equation yielding $V_r(R)$ **(or** $Y(R)$**)**, we find that the wind acceleration decreases as μ increases so that V_* decreases and the Alvén radius must increase. Physically, this increase in the Alfvén radius is due to a less efficient acceleration mechanism. The analysis and clear understanding of this result is complicated by the fact that as μ changes there is a direct effect on the radial magnetic field but also on the radial velocity latitudinal profile and, indirectly, the wind pressure and temperature. Therefore, the increase in angular momentum cannot be solely attributed to the increase of magnetic field concentration as this cannot be separated from changes in other physical quantities. This result is at odds with the result of Sect. 2 where no significant difference in angular momentum loss as a function of field concentration was found. This discrepancy may be explained by the fact that the two models address totally different scenarios characterized by different plasma β regimes.

4. Discussion

Empirical or qualitative models of magnetized stellar winds have been very successful in establishing the basic physical principles that govern the rate of angular momentum loss associated with a wind. In particular, the work of Mestel (1968) and Mestel & Spruit (1987) investigates how the magnetic braking efficiency varies with stellar rotation rate. It shows that it is possible to have saturation in the angular momentum loss rate with rotation without dynamo saturation as a result of two competing effects. On the one hand, the magnetic torque increases with rotation rate due to the increase of the field strength. On the other hand, the fraction of the stellar surface with open magnetic field lines contributing to braking decreases with rotation rate. This model has also been applied to establish that a rearrangement of the surface field from a low order to a high order multipole at high rotation rates implies a decrease in braking efficiency (Taam & Spruit 1989).

There are, however, limitations to how much information can be obtained from these qualitative models. In this work, we simply address the question of whether a correct estimate of the influence of the magnetic surface field concentration towards the poles can be obtained using these empirical models or whether such a goal requires a computation of the field that takes into account force balance in all directions. To this end, in Sect. 2 we determine the coronal magnetic field due to a surface flux distribution concentrated around the poles and show that this distribution is not maintained further out. Instead, the magnetic field rapidly expands to regions of low magnetic pressure and approaches the simple split-monopole field. Flux tubes at different latitudes have very different expansion rates, but we find that this has no significant effect on the angular momentum transported outwards.

In order to investigate the properties of stellar winds for different surface flux distributions we apply, in Sect. 3, the analytical wind model of Lima et al. (2001). To our knowledge, this is the first application of an analytical quantitative 2D model to the problem of magnetic braking in young solar- type stars. This model has very appealing characteristics has it describes the outflow of a rotating star for which the latitudinal magnetic flux distribution is the same at all radial distances. It also has some limitations that are typical of this kind of model. It is constructed under the assumption of separation of variables and there is no energy equation, with the temperature being determined from the perfect gas law. Also, although the model allows different surface flux distribution, its range of variation is somewhat limited. Its most restrictive properties, however, are that the Alfvén surface is spherical, contrary to what is expected for fast rotators and has been proposed by Solanki et al. (1997), and the absence of meridional components of the velocity and magnetic field. Therefore, the conclusions obtained from using this model cannot be a priori considered as general features. Yet, some of the results are extremely relevant as they convey fundamental physical principles. We find that the surface concentration of magnetic flux at high latitudes can only occur in the corona for a relatively high plasma beta, so that the gas pressure gradient

can oppose the Lorentz force that tends to bend the field lines towards the equator. This work stresses the importance of the latitudinal profiles of the physical quantities involved in the description of the hydro-magnetic wind. As shown in Sect. 3.2, the radial features of the wind, such as the acceleration mechanisms, are not only dependent on the force balance along the lines but also on the force balance across the lines. Furthermore, a given radial field latitudinal profile implies, due to force balance and under the assumptions of the model, a certain latitudinal profile of the density and velocity that are as important as the magnetic field in determining the angular momentum loss rate. The most important prediction from this model is that a higher polar field concentration leads to larger braking rates than a smoother field distribution. However, because of the inherent coupling of this result with some of the assumptions of the model, this cannot be viewed as general. In spite of this, we have presented an example of an equilibrium model, with unknown stability properties, for which magnetic braking increases as the field concentration to the pole increases. Remarkably, this model has the attractive property of having a magnetic topology identical to the models of Holzwarth (2005), Holzwarth & Jardine (2006) and Solanki et al. (1997) but it complies with force balance in all directions, which generates antagonistic results.

Both models presented in this work neglect the poleward collimation of the field lines characteristic of FMR. An interesting question is whether this poleward collimation increases or decreases the angular momentum loss of the star, but we are not aware of any work specifically addressing this issue. At high latitudes R_* increases due to the effect of collimation but the opposite happens near the equator (e.g. Sakurai 1985), so that the end result depends on which effect is dominant. In Sect. 2 we have determined that at 4–8 stellar radii from the stellar surface the radial field becomes uniform in latitude, independently of its surface distribution, and that in general this occurs very much inside the Alfvén surface. Therefore, we expect that field collimation would occur identically for both uniform and highly concentrated surface field distributions with no significant differences in angular momentum loss.

Based on the results presented in Sects. 2 and 3, we argue that the concentration of magnetic flux at high latitudes does not directly contribute to limit the braking efficiency of the wind. By comparing the results obtained with the two different models one could in principle be able to infer how crucial the limitations introduced are in the analytical treatment of the 2D model to the results obtained. The extent to which this comparison can be made is limited by the very different assumption about the plasma β in the two cases. We hypothesize that the increase in angular momentum loss with magnetic field concentration observed in Sect. 3 results from changes in the gas temperature, density and pressure that are generated to maintain force balance across the field in the absence of meridional components. One can speculate about what to expect if some of the most stringent assumptions of our 2D model are relaxed. We suggest that allowing for meridional components, non spherical Alfvén surface and a more realistic plasma β would lead to closed magnetic field lines near the equator. Furthermore, a surface field concentrated towards the pole would have a weaker field at low latitudes and consequently have more open magnetic flux than a smooth surface magnetic field. This would again imply larger braking rates for a surface field concentrated towards the pole than for a smooth field with equal amounts of magnetic flux, if the wind properties are similar in the two cases. However, the existence of large amounts of magnetic flux at high latitudes can still lead to a reduced angular momentum loss rate if it creates a complex field topology akin to multi-order magnetic fields (cf. Taam & Spruit 1989).

The work presented here can be extended by further analytical modelling or numerical simulations. However, many aspects are still unknown and this constrains how much one can predict about magnetic braking. It is still not known whether polar spots are largely unipolar, as assumed here (for opposing views see e.g. Schrijver & Title 2001; McIvor et al. 2003). In addition, we cannot rule out the possibility that stellar winds are accelerated by dissipation of magnetic waves as well as thermal and centrifugal forces. The nature of the slow solar wind is still largely unknown and it remains an open question whether it is admissible to ignore the contribution of the slow wind to the angular momentum evolution of active late-type stars.

5. Conclusions

In the present work we investigate how the magnetic surface field distribution affects the coronal magnetic field and the rate of angular momentum removal by the stellar wind.

There are three important results from our work: first, we have shown that very different surface flux distributions yield similar coronal fields in a low β coronal plasma as well as similar wind braking rates. Second, we have demonstrated that the radial features of the wind, such as the acceleration mechanisms and the gas pressure distribution, are not only dependent on the force balance along the field lines, but also on the force balance across the field lines. Finally, in the wind model of (Lima et al. 2001) a higher polar field concentration leads to larger braking rates than a smoother field distribution. However, we cannot rule out the possibility that this is a result of the assumptions of the model and so it may not be regarded as a general feature. This model also demonstrates that the rate of braking is dependent on the latitudinal behaviour of several physical quantities and not only of the surface radial field.

We conclude that the concentration of magnetic flux at high latitudes is unlikely to directly constrain the braking efficiency of the wind. It may, however, have a decisive importance in determining the amount of open magnetic flux that contributes to wind magnetic braking.

Acknowledgements. This work was partially supported by grant POCI/CFE-AST/55691/2004 approved by FCT and POCI, with funds from the European Community program FEDER. J. M. Ferreira wishes to thank Volkmar Holzwarth for a profitable exchange of ideas during Cool stars XIV. The authors would like to thank the Referee for several useful suggestions and references on the corona and solar wind.

Appendix A: Stream functions

Here we give the explicit forms of Z_n for $n = 5$ and $n = 7$:

$$\begin{aligned} Z_5 \;=\; & \frac{15}{14} r \left(1 - v^2\right)\left(21v^4 - 14v^2 + 1\right) \\ & \times \left[15\left(1 + u^2\right)\left(1 + 14u^2 + 21u^4\right)\tan^{-1}\frac{1}{u}\right] \\ & - \frac{225}{16}\frac{\pi a^2}{r}\sin^2\theta - \frac{1675}{32}\frac{\pi a^4}{r^2}\sin^2\theta\left(5\cos^2\theta - 1\right) \\ & - \frac{4725}{128}\frac{\pi a^6}{r^5}\sin^2\theta\left(1 - 14\cos^2\theta + 21\cos^4\theta\right) \\ & + 30a\eta \end{aligned} \tag{A.1}$$

$$
\begin{aligned}
Z_7 \;=\; & \frac{7}{16} r\left(1-v^2\right)\left(429v^6-495v^4+135v^2-5\right) \\
& \times\left[\left(429u^6+495u^4+135u^2+5\right)\tan^{-1}\frac{1}{u}\right. \\
& \left.+\frac{1}{80}\left(1837u+14273u^3+27335u^5+15015u^7\right)\right] \\
& +\frac{3}{4}\frac{\pi a^2}{r}\sin^2\theta+\frac{6615}{32}\frac{\pi a^4}{r^3}\sin^2\theta\left(5\cos^2\theta-1\right) \\
& +\frac{8085}{2}\frac{\pi a^6}{r^5}\sin^2\theta\left(1-14\cos^2\theta+21\cos^4\theta\right) \\
& +\frac{21021}{512}\frac{\pi a^8}{r^5}\sin^2\theta\left(-5+135\cos^2\theta-495\cos^4\theta\right. \\
& \left.+429\cos^6\theta\right)+56a\eta, \qquad \text{(A.2)}
\end{aligned}
$$

with

$$
u^2=-\frac{1}{2}\left(1-\frac{a^2}{r^2}\right)+\frac{1}{2}\left[\left(1-\frac{a^2}{r^2}\right)^2+\frac{4a^2}{r^2}\cos^2\theta\right]^{1/2}, \qquad \text{(A.3)}
$$

$$
v^2=-\frac{1}{2}\left(\frac{a^2}{r^2}-1\right)+\frac{1}{2}\left[\left(\frac{a^2}{r^2}-1\right)^2+\frac{4a^2}{r^2}\cos^2\theta\right]^{1/2}, \qquad \text{(A.4)}
$$

$$
\eta^2=-\frac{1}{2}\left(\frac{r^2}{a^2}-1\right)+\frac{1}{2}\left[\left(\frac{r^2}{a^2}-1\right)^2+\frac{4r^2}{a^2}\cos^2\theta\right]^{1/2}. \qquad \text{(A.5)}
$$

Appendix B: Wind model

Here we present how the wind solution is obtained. As we follow very closely the approach of Sakurai (1985), only a brief description is given. We assume azimuthal symmetry and by combining the equations of mass and magnetic flux conservation, the frozen-in condition, the polytropic law and the momentum conservation equation in the poloidal and azimuthal directions we arrive at a Bernoulli integral of the equation of motion

$$
\begin{aligned}
H \;=\; & \frac{v_{\rm p}^2}{2}-\frac{\Omega^2(r_*\sin\theta)^2}{2}\left[\left(\frac{\frac{r_*}{r}-\frac{r}{r_*}}{\frac{\rho}{\rho_*}-1}\right)^2-\left(\frac{r}{r_*}\right)^2\right] \\
& +\frac{\gamma}{\gamma-1}\frac{p}{\rho}-\frac{GM}{r}=E, \qquad \text{(B.1)}
\end{aligned}
$$

where $v_{\rm p}$ is the poloidal velocity, Ω the stellar angular velocity, M the mass of the star, G the gravitational constant, E an integration constant and the subscript $*$ stands for the Alfvén point. Upon applying the law of mass conservation, $\rho V_{\rm p} S = \rho_0 V_{\rm p_0} S_0$, with S representing the area of the flux tube and the subscript 0 the values at the stellar surface, we obtain $H = H(r,\rho)$. At the fast and slow critical points one has the regularity conditions

$$
\frac{\partial H}{\partial \rho}=\frac{\partial H}{\partial r}=0, \qquad \text{(B.2)}
$$

together with

$$
H(r_s,\rho_s)=H(r_f,\rho_f)=E. \qquad \text{(B.3)}
$$

Applying mass and flux conservation allows us to write the density at the Alfvén point as

$$
\rho_*=\rho_0\frac{V_0^2}{V_{A_0}^2}. \qquad \text{(B.4)}
$$

The system of six simultaneous algebraic Eqs. ((B.2), (B.3)) is solved for the unknowns r_*, $r_{\rm s}$, $\rho_{\rm s}$, $r_{\rm f}$, $\rho_{\rm f}$ and v_0. The integration constant E is not an additional unknown as it can be written in terms of V_0 and r_*. We note that, contrary to Sakurai (1985), we solve our equations in dimensionless form with respect to surface values and not with respect to the Alfvén radius as, in general, $S \propto r^2$ does not hold.

References

Altschuler M. D., & Newkirk, Jr. G. 1969, Sol. Phys., 9, 131
Balogh A., Smith E. J., Tsurutani B. T., et al. 1995, Science, 268, 1007
Barnes S., & Sofia S. 1996, ApJ, 462, 746
Barnes J. R., Collier Cameron A., Unruh Y. C., Donati J. F., & Hussain G. A. J. 1998, MNRAS, 299, 904
Belcher J. W., & MacGregor K. B. 1976, ApJ, 210, 498
Buzasi D. L. 1997, ApJ, 484, 855
Collier Cameron A., & Robinson R. D. 1989, MNRAS, 236, 57
Collier Cameron A., & Donati J. F. 2002, MNRAS, 329, L23
Cranmer S. R. 2005, in ESA SP-592: Solar Wind 11/SOHO 16, Connecting Sun and Heliosphere
Donati J. F., Collier Cameron A., Hussain G. A. J., & Semel M. 1999, MNRAS, 302, 437
Heyvaerts J., & Norman C. A. 1989, ApJ, 347, 1055
Holzwarth V. 2005, A&A, 440, 411
Holzwarth V., & Jardine M. 2005, A&A, 444, 661
Holzwarth V., & Jardine M. 2006, ArXiv Astrophysics e-prints
Hussain G. A. J., Jardine M., & Collier Cameron A. 2001, MNRAS, 322, 681
Keppens R., & Goedbloed J. P. 1999, A&A, 343, 251
Lepeltier T., & Aly J. J. 1996, A&A, 306, 645
Li J. K., Wu K. W., & Wickramasinghe D. T. 1994, MNRAS, 270, 769
Lima J. J. G., Priest E. R., Tsinganos K. 2001, A&A, 371, 240
Low B. C. 1986, ApJ, 310, 953
MacGregor K. B., & Brenner M. 1991, ApJ, 376, 204
McIvor T., Jardine M., Cameron A. C., Wood K., & Donati J. F. 2003, MNRAS, 345, 601
Mestel L. 1968, MNRAS, 138, 359
Mestel L., & Spruit H. C. 1987, MNRAS, 226, 57
Parker E. N. 1979, Cosmical Magnetic Fields, The International Series of Monographs on Physics, (New York: Oxford University Press)
Riley P., Linker J. A., Mikić Z., et al. 2006, ApJ, 653, 1510
Sakurai T. 1985, A&A, 152, 121
Sauty C., & Tsinganos K. 1994, A&A, 287, 893
Schatzman E. 1962, Ann. Astrophys., 25, 18
Schmitt J. H. M. M., & Favata F. 1999, Nature, 401, 44
Schrijver C. J., Title A. M. 2001, ApJ, 551, 1099
Schuessler M., & Solanki S. K. 1992, A&A, 264, L13
Smith E. J., & Balogh A. 1995, Geophys. Res. Lett., 22, 3317
Solanki S. K., Motamen S., Keppens R. 1997, A&A, 325, 1039
Strassmeier K. G. 2002, Astron. Nachr., 323, 309
Strassmeier K. G. 2005, Astron. Nachr., 326, 269
Suess S. T., & Smith E. J. 1996, Geophys. Res. Lett., 23, 3267
Suess S. T., Richter A. K., Winge C. R., & Nerney S. F. 1977, ApJ, 217, 296
Taam R. E., & Spruit H. C. 1989, ApJ, 345, 972
Tsinganos K., Sauty C., Surlantzis G., Trussoni E., & Contopoulos J. 1996, MNRAS, 283, 811
Tsinganos K., & Trussoni E. 1991, A&A, 249, 156
Vogt S. S., & Penrod G. D. 1983, PASP, 95, 565
Weber E. J., & Davis L. J. 1967, ApJ, 148, 217